

Cell Reports, Volume 35

Supplemental information

**Contiguous erosion of the inactive X
in human pluripotency concludes
with global DNA hypomethylation**

Prakhar Bansal, Darcy T. Ahern, Yuvabharath Kondaveeti, Catherine W. Qiu, and Stefan F. Pinter

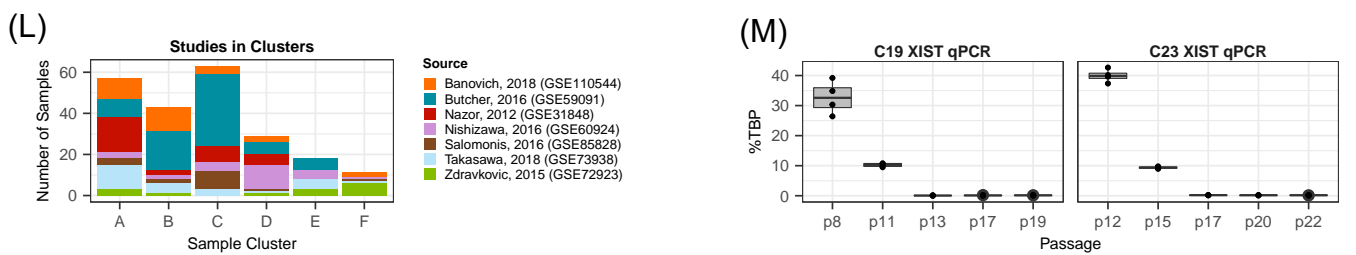
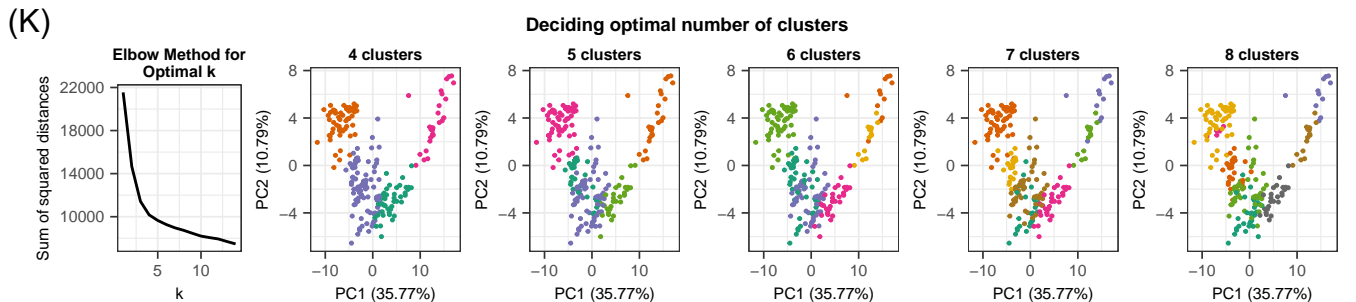
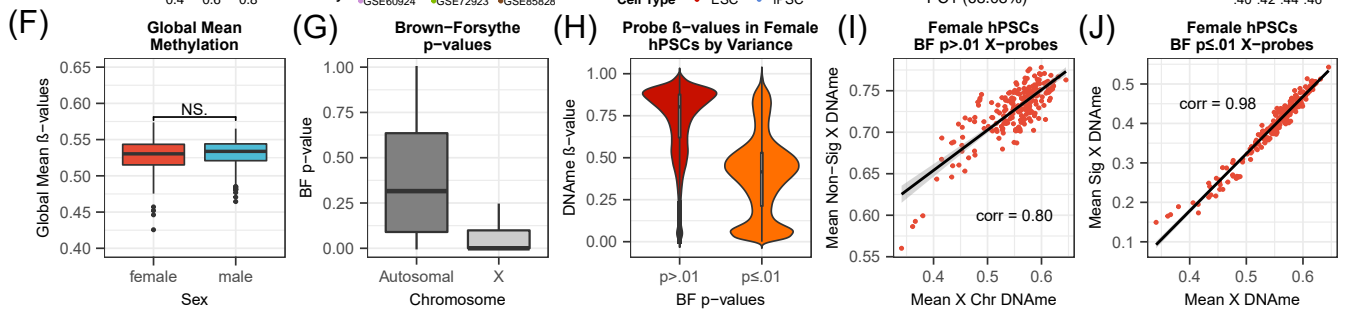
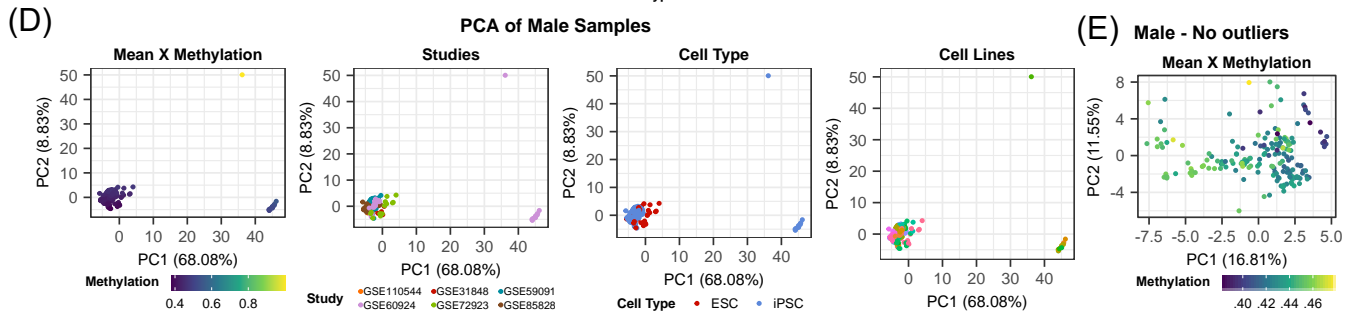
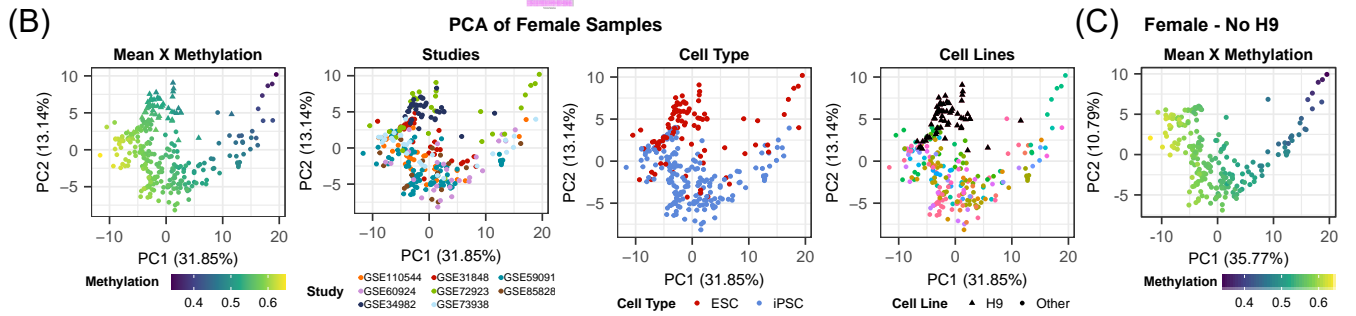
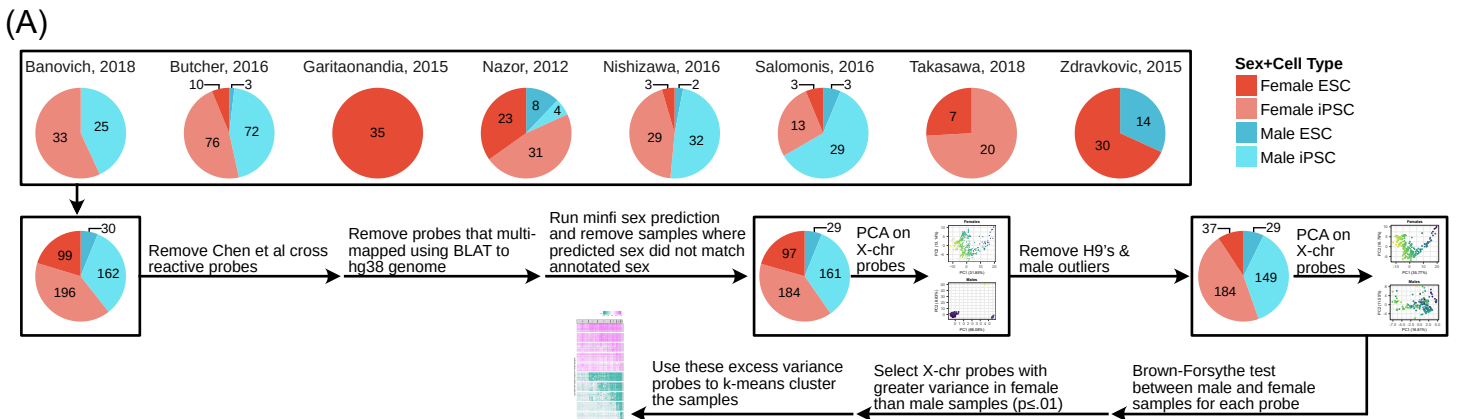


Fig S1. Data processing and outlier identification. Related to Figure 1 and methods about “Data Collection, Processing, and Normalization”.

(A) Schematic of filtering and processing pipeline for DNA methylation data.

(B) and (C) PCAs of female samples on all X-probes before and after H9 removal, respectively. Plots are colored by different properties of the samples as indicated by the legends.

(D) and (E) PCAs of male samples on all X-probes before and after outlier removal, respectively. The plots are colored by different properties of the samples as indicated by the legends.

(F) Global mean methylation for female and male samples (N.S. = not significant).

(G) Brown-Forsythe test p-values for autosomal probes and X-probes showing that X-probes are significantly more variant between the male and female samples than autosomal probes.

(H) Distribution of β -values for X-probes that are more variant in female samples ($p \leq .01$), and those that are not ($p > .01$).

(I) and (J) Relationship between the mean X chromosome methylation and mean methylation of X-probes above or below the BF-test p-value cutoff (.01), respectively. The line shows the linear regression, and “corr” is the Pearson correlation.

(K) Plots of the elbow method to find the appropriate number of clusters for the k-means clustering of female samples.

(L) Breakdown of sample clusters by study of origin.

(M) XIST qPCR for C19 and C23 iPSCs. Each passage has one sample with 4 technical replicates each.

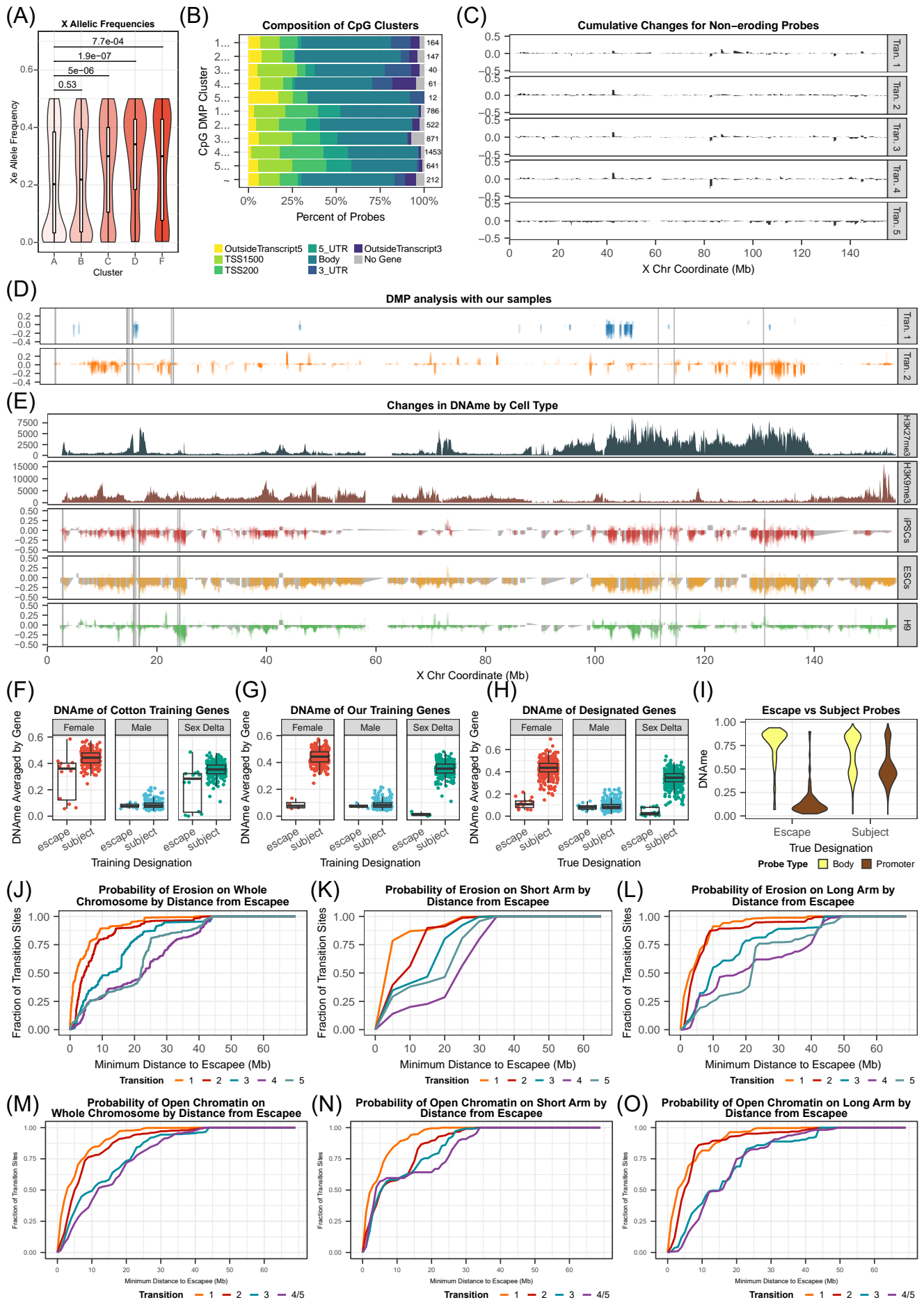
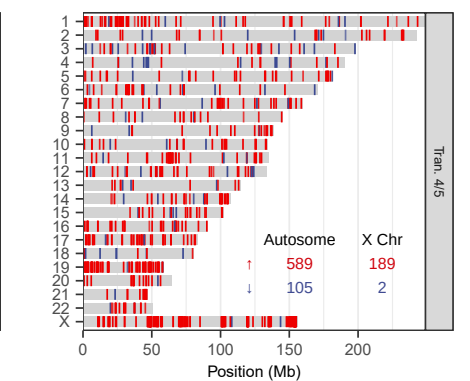
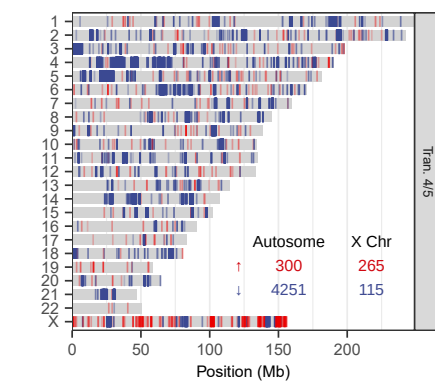
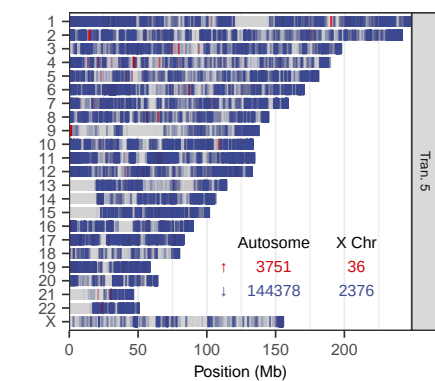
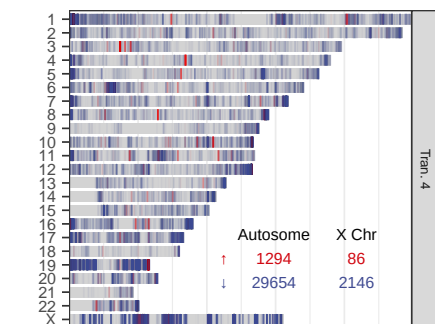
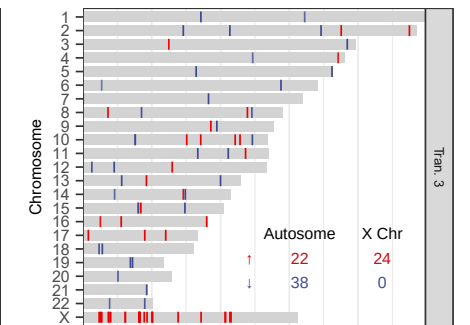
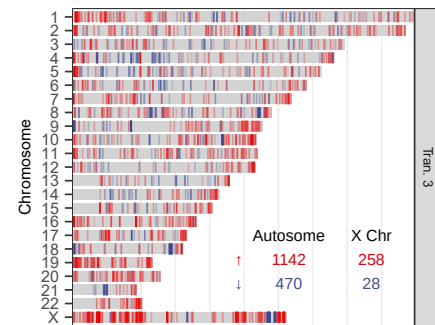
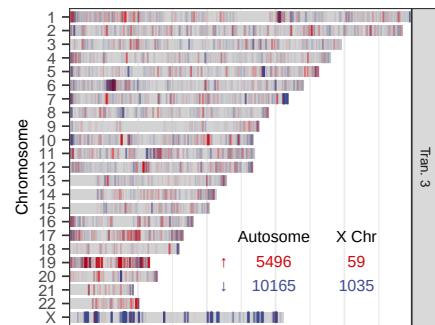
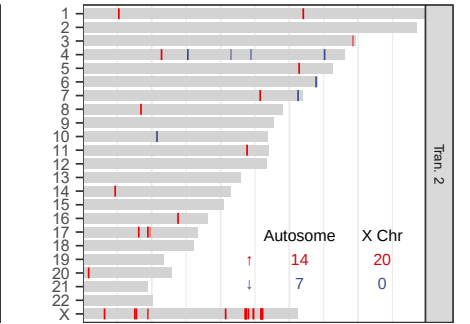
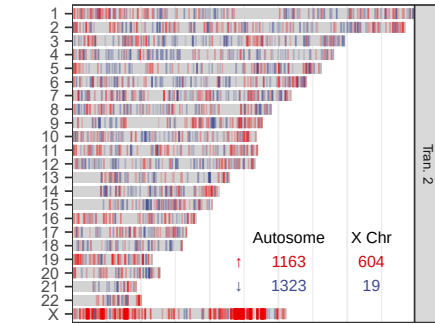
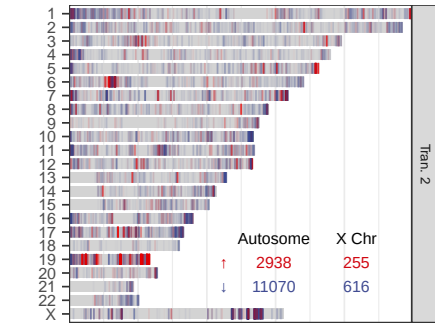
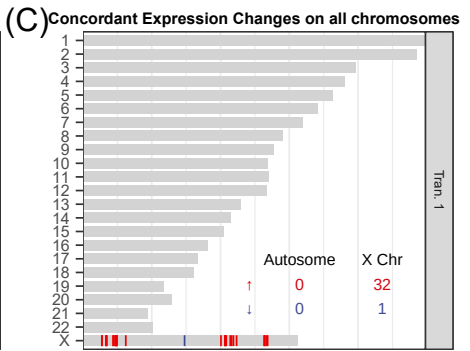
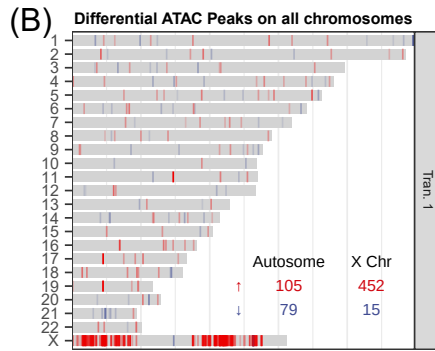
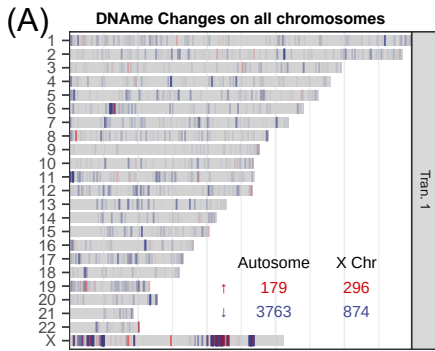


Fig S2. DNAm dynamics during XIE distinguish escapees and reactivated genes. Related to Figure 3 and methods about “Annotating Genes as Escapees” and “Calculating distances to escapee genes.”

- (A) Distribution of allele frequencies of the Xe as inferred by the lesser allele fraction for each RNA-seq hPSC sample across heterozygous positions (Wilcoxon test p-values relative to cluster A).
- (B) Percent composition of DMPs in each probe group from Figure 2A, as described in the methods. Probe totals for each group are listed to the right.
- (C) Cumulative changes through each transition for X-linked probes with high sex-variance but without consistent direction across transitions (“~” symbol), plotted as in Fig. 3A.
- (D) Changes in DNAm based on DMP analysis with C19 and C23 samples only. Changes for transition specific probes are shown (similar to Fig 3A) in relation to cluster A C19 and C23 samples. Correlation to meta-analysis transition-specific DMPs is shown in top-right.
- (E) Changes in DNAm (similar to Fig 3A) separated by whether the sample is an iPSC, ESC, or H9. All comparisons are to cluster A samples.
- (F-H) Identification of escapees using the Cotton et al method. “Sex Delta” panels show the difference in methylation for a gene between male and female samples. (E) methylation values of the initial Cotton, et al. trainee genes, (F) as G after removal of initial trainee genes that fail cutoffs (as in Cotton et al), and (G) final escapee gene set after true designation is determined and the escapees are identified.
- (I) Distribution of β -values of gene body and promoter probes for escapees and genes subject to XCI.
- (J) Cumulative probability of CpG demethylation in each transition as a function of distance to escapee genes on the whole X chromosome.
- (K) as in J, for CpGs on Xp.
- (L) as in J, for CpGs on Xq.
- (M) Cumulative probability of ATAC-peak openings in each transition as a function of distance to escapee genes on the whole X chromosome.
- (N) as in M, for ATAC-peaks on Xp.
- (O) as in M, for ATAC-peaks on Xq.



Direction of Change — Decreasing — Increasing
abs(delta) 0.00 — 0.25 — 0.50

Direction of Change — Decreasing — Increasing
abs(log2FC) — 1 — 2 — 3 — 4

abs(log2FC) — 0.00 — 0.25 — 0.50
Direction of Expression Change — Decreasing — Increasing

Fig S3. Global changes in DNAm and gene expression. Related to Figure 4 and methods about “Concordance and Enrichment Analysis.”

(A) Chromosome-resolved DMPs assigned to specific transitions by p-value. Total counts for autosomal and X chromosome probes are provided, with direction of change indicated (blue = loss of DNAm, and red = gain of DNAm). The transparency is on a continuous scale based on the β -differential.

(B) Chromosome-resolved differential ATAC peaks assigned to specific transitions by FDR. Total counts are provided as for (A) (blue = closing ATAC peak, red = opening ATAC peak). The transparency is on a continuous scale based on the $\log_2(\text{fold change})$ of the ATAC peaks.

(C) Chromosome-resolved differentially expressed genes concordant with either DMP (A) or differential ATAC peaks (B). Total counts are provided as for (A) (blue = decreasing expression, and red = increasing expression). The transparency is on a continuous scale based on the $\log_2(\text{fold change})$ of the expression.

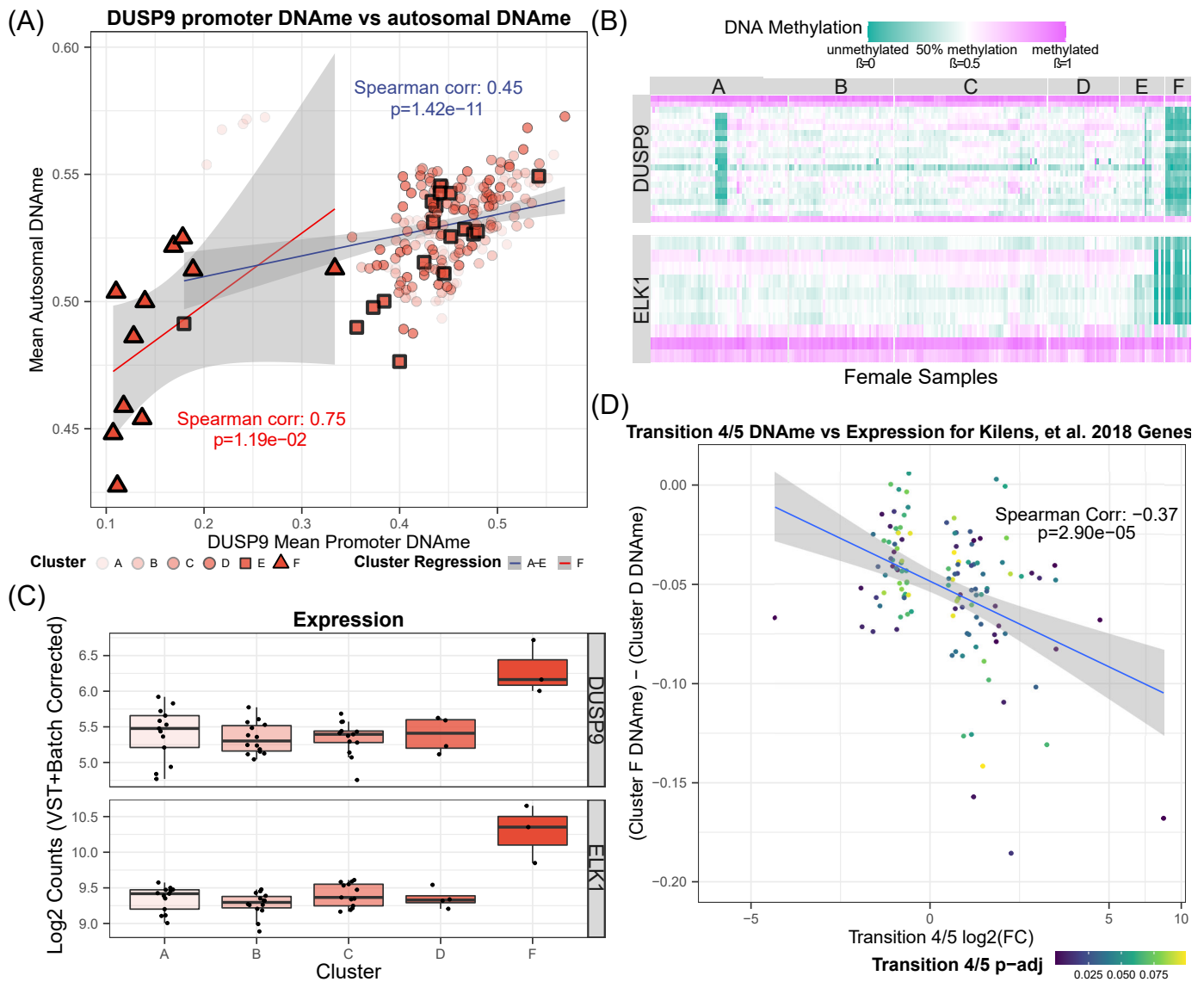


Fig S4. Autosomal DNAm changes relative to DUSP9 reactivation impact naïve markers. Related to Figure 4.

(A) Relationship of DUSP9 promoter methylation to autosomal methylation in female samples. Clusters E and F are emphasized to highlight the change in global and DUSP9 methylation in the last transition.

(B) DNAm heatmap of DUSP9 and ELK1 probes across clusters A-F.

(C) DUSP9 and ELK1 (VST+batch-corrected/log2-transformed) expression across clusters A-F.

(D) Change in methylation for genes that are differentially expressed in Transition 4/5 and are differentially expressed in naïve stem cells (Kilens et al., 2018).